Journal of Ceramic Processing Research. Vol. 27, No. 1, pp. 168~175 (2026)
(Received 19 April 2025, Received in revised form 8 July 2025, Accepted 14 August 2025)
https://doi.org/10.36410/jcpr.2026.27.1.168

J O U R N A L O F
Ceramic Processing Research

Research and characterization of porous ceramic materials prepared from solid waste

Yan Zhou[a,b,c], Xin Zhu[b,c] and Jiao Yan[b,c,*]
[a]*East China University of Science and Technology, Shanghai, 200237, China*
[b]*Key Laboratory of Soil and Groundwater Pollution Prevention, Control and Green Remediation of Sinopec, Ltd, Guangzhou 510000, Guangdong, China*
[c]*Sinopec Fifth Construction Co.Ltd. Guangzhou 510000, Guangdong, China*

With the advancement of industrialization and urbanization, the sharp increase in solid waste has led to severe environmental challenges, making its resource utilization a prominent research focus. In this study, sludge, gasification slag, shale, glass wool, and waste alkali solution were selected as raw materials to prepare porous ceramic materials through processes such as drying, mixing, ball milling, molding, and high-temperature sintering. The effects of material ratios, sintering temperature, and sintering time on the performance of the porous ceramics were systematically investigated. Analytical techniques such as X-ray diffraction (XRD) and scanning electron microscopy (SEM) were employed to examine the phase composition and microstructure. The results show that when the ratio of sludge, gasification slag, glass wool, shale, and waste alkali solution is 5:2:1:1:1, the sintering temperature is 1100 °C, and the holding time is 4 hours, the prepared porous ceramics exhibit excellent performance. The samples demonstrated favorable properties such as apparent porosity and flexural strength, with stable phase composition and well-developed microstructure. This research opens a new pathway for the resource utilization of solid waste, offering significant environmental and economic benefits, and holds great potential to promote development in related fields.

Keywords: Solid waste, Resource utilization, Porous ceramics, Material characterization.

Introduction

With the rapid acceleration of industrialization and urbanization in China, the generation of solid waste has been increasing significantly, making its disposal one of the most pressing environmental challenges faced globally [1]. The vast quantities of solid waste not only occupy large areas of land but also cause severe and often irreparable damage to soil, water bodies, and the atmosphere. This poses a serious threat to ecological balance and human health and survival [2]. Therefore, how to convert large volumes of solid waste into reusable resources has become a critical consideration for sustainable development and a key pillar for supporting human health and well-being [3]. In this context, the development of effective technologies for the resource utilization of solid waste holds great practical significance and has become a major focus in the fields of environmental science and materials science.

Porous ceramic materials, due to their unique pore structures, possess numerous outstanding properties such as low density, high specific surface area, excellent adsorption capacity, permeability, and chemical stability [4]. These characteristics grant them broad application prospects in areas such as filtration, separation, catalysis, thermal insulation, and biomedicine [5]. Traditionally, the production of porous ceramics has relied on high-purity raw materials, which not only leads to high manufacturing costs but also places significant strain on natural resources. In recent years, increasing research attention has been devoted to the use of solid waste as raw material for producing porous ceramics [6]. This approach not only enables the reduction and harmless treatment of solid waste but also helps lower the production costs of porous ceramics, offering a new pathway for solid waste valorization with considerable economic and environmental benefits.

This study utilizes sludge, gasification slag, shale, glass wool, and waste alkali solution as raw materials. By analyzing the physicochemical properties and phase composition of these solid wastes, and employing characterization techniques such as XRD and SEM, the research explores the feasibility of producing porous ceramic materials and methods for optimizing their performance. It aims to reveal the intrinsic relationship between the composition of solid waste and the properties of porous ceramics. The goal is to provide a solid theoretical foundation and feasible technical support

*Corresponding author:
Tel : 17370043397
Fax: 020-28348128
E-mail: 1425631710@qq.com

for the industrial application of porous ceramics derived from solid waste, promote the advancement of solid waste utilization technologies, and contribute to solving solid waste disposal challenges and the development of new environmentally friendly materials.

Materials and Methods

Experimental Materials

The sludge used in the experiment was collected from a municipal wastewater treatment plant. The gasification slag, glass wool, shale, and waste alkali solution were sourced from a petrochemical site. The chemical compositions of these materials are shown in Table 1, and the XRD analysis results are presented in Fig. 1. As indicated in Table 1, the primary components of the four raw materials are SiO_2, Al_2O_3, and Fe_2O_3, with minor amounts of other metal oxides such as CaO and K_2O. According to Fig. 1, the main crystalline phases in the sludge are quartz (SiO_2) and calcite ($CaCO_3$). The mineral composition of the gasification slag primarily includes quartz (SiO_2) and ferric oxide (Fe_2O_3). The glass wool mainly consists of amorphous glassy substances, which appear as broad diffuse peaks in the XRD pattern, along with a small number of crystalline impurity peaks. The main crystalline phases in the shale are quartz (SiO_2), feldspar minerals, and carbonate mineral phases.

Sample Preparation

Preparation of Porous Ceramics

The preparation process of porous ceramic materials is illustrated in Fig. 2. First, the raw sludge is dried and then mixed with gasification slag, glass wool, shale, and waste alkaline solution in a specified ratio. The mixture is ball-milled at a speed of 600 $r \cdot min^{-1}$ for 30 minutes and passed through a 200-mesh sieve. A certain proportion of waste alkaline solution is then added to the sieved mixture, which is thoroughly stirred and poured into

Table 1. Chemical composition of raw materials (W/%).

Raw materials	SiO_2	Al_2O_3	Fe_2O_3	CaO	MgO	K_2O	TiO_2
gasification slag	50.5	17.78	12.27	7.89	3.78	2.45	1.08
sludge	40.72	14.78	9.63	8.51	6.12	3.38	0.76
glass wool	72.16	2.17	1.52	8.59	5.19	0.57	0.29
shale	58.15	24.67	8.10	0.65	1.37	1.38	1.25

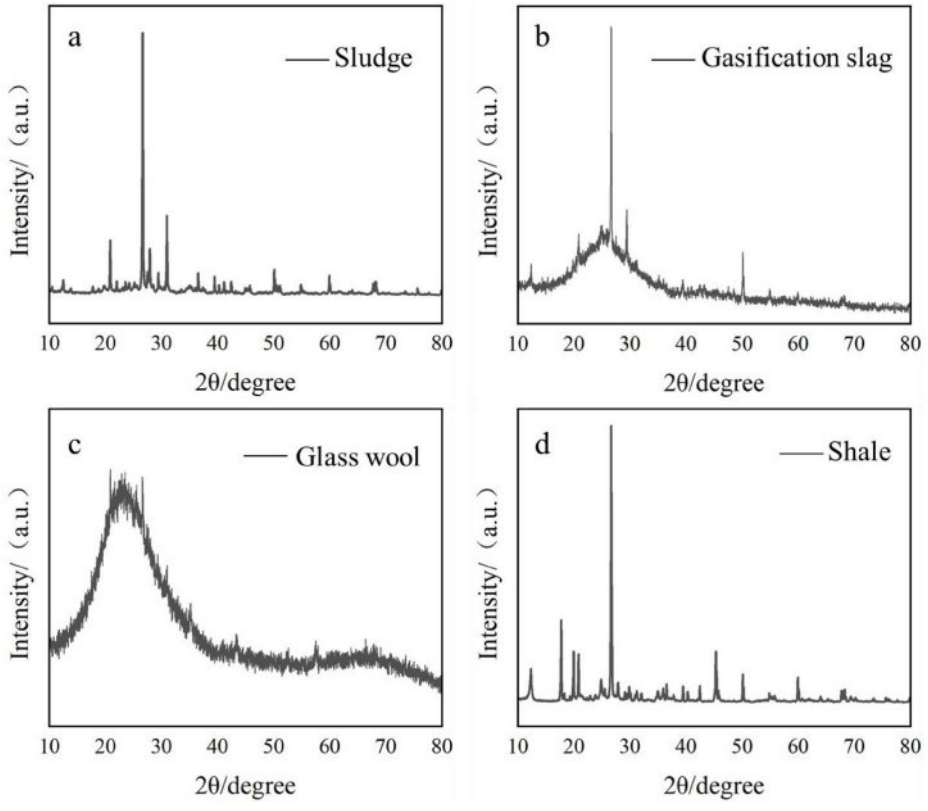

Fig. 1. XRD diffraction pattern of raw materials (Note: The original data has been provided via email.)

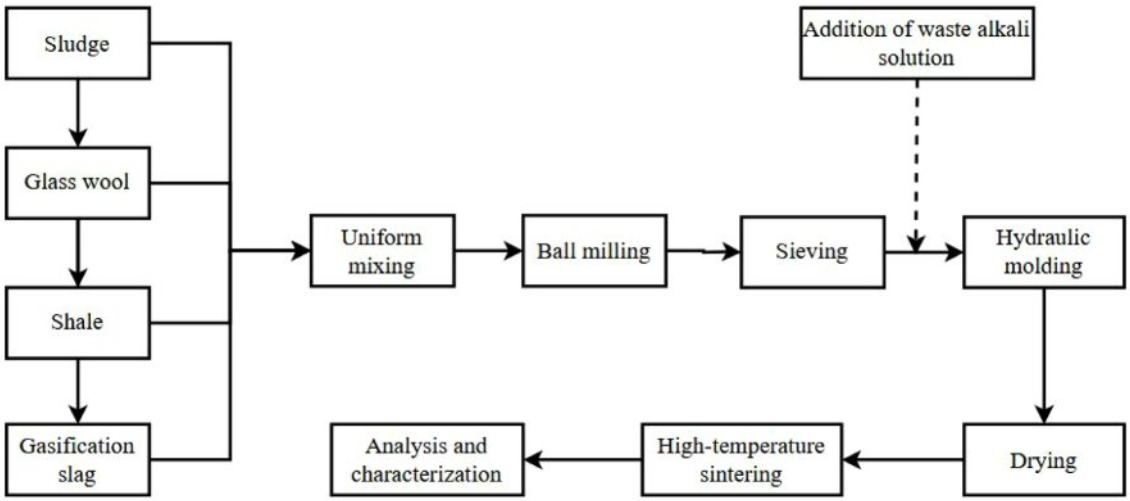

Fig. 2. Flow chart of porous ceramics preparation.

Table 2. Raw material ratio.

Group number	Sludge /%	Gasification slag /%	Glass wool /%	Shale /%	Waste alkali solution /%
A1	60	10	10	10	10
A2	50	20	10	10	10
A3	45	20	15	10	10
A4	40	20	20	10	10

a pressing mold. The mixture is hydraulically pressed into a disc shape under a forming pressure of 10 MPa, maintained for 20 seconds. Finally, the formed samples are placed in a roller kiln for high-temperature sintering, resulting in the production of porous ceramic materials (Table 2).

Characterization of Porous Ceramics

The apparent porosity and water absorption of the porous ceramics were measured according to the "Determination of Apparent Porosity and Bulk Density of Porous Ceramics" (GB/T 1966-2024). The chemical composition of the raw materials was analyzed using X-ray fluorescence (XRF) spectroscopy. The phase composition of both the raw materials and the prepared porous ceramics was analyzed using X-ray diffraction (XRD) with CuKα radiation, scanned over the 10–80° range. The microstructure of the porous ceramics was examined using scanning electron microscopy (SEM) [11].

Results and Discussion

Effects of Different Ratios on the Properties of Porous Ceramics

Figure 3 illustrates the effects of different raw material ratios on the apparent porosity, water absorption, compressive strength, and bulk density of porous ceramics. Fig. 3a shows the apparent porosity under various raw material ratios. As observed, when the raw material ratio is A2, the apparent porosity of the porous ceramic reaches 67.89%. The balanced composition in group A2 effectively regulates the ratio between the solid and liquid phases, retaining a three-dimensional interconnected pore structure while enhancing mechanical strength through the formation of a silicate network. Additionally, the waste alkaline solution acts as a binder, and its alkaline components promote the low-temperature eutectic reaction between SiO_2 and Al_2O_3 in the raw materials, thereby reducing the sintering activation energy [12]. Fig. 3b presents the water absorption under different raw material ratios. When the ratio is A2, the water absorption of the porous ceramic is 59.57%. The trend in water absorption closely follows that of apparent porosity, due to the fact that sludge, shale, and glass wool leave behind pores during the high-temperature sintering process, forming channels that increase the internal porosity of the ceramic and result in a looser structure, which in turn facilitates water absorption. Fig. 3c shows the compressive strength of the porous ceramics under various raw material ratios. It can be seen that with increasing raw material ratio, the compressive strength initially decreases and then increases. This trend is consistent with the variation in bulk density shown in Fig. 3d. The increase in oxide content within the raw materials leads to a higher amount of liquid phase generated during sintering, which clogs some of the pores. Consequently, the bulk density increases and the compressive strength is improved.

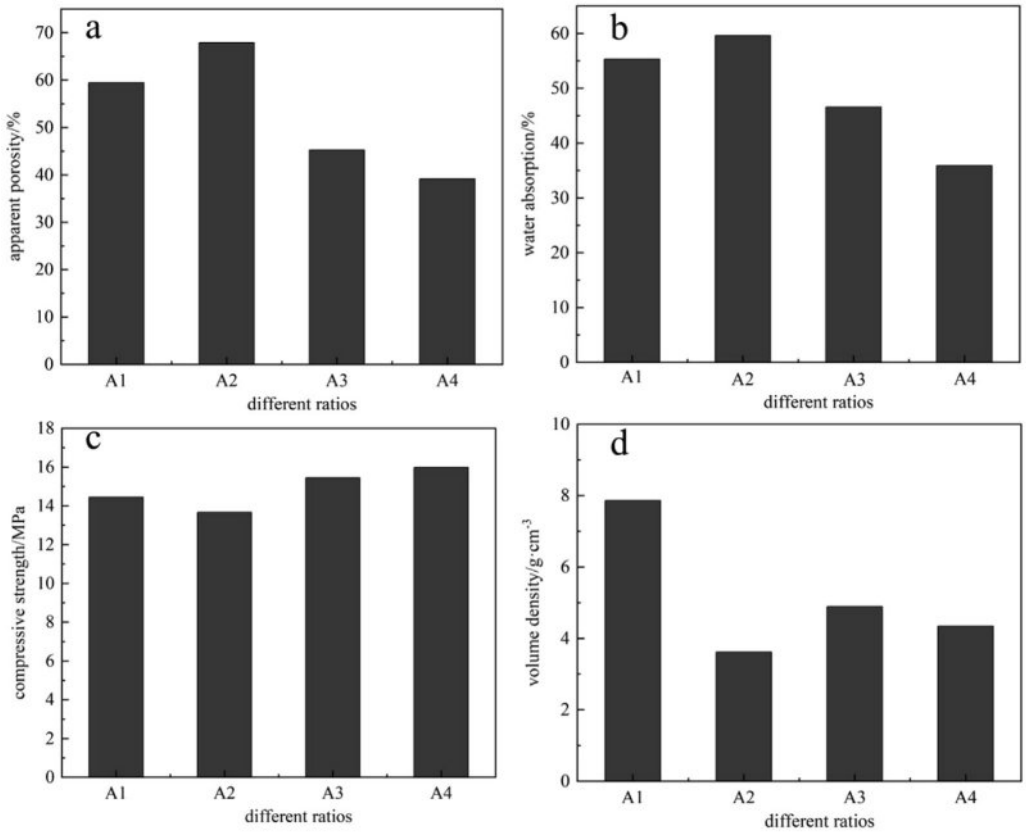

Fig. 3. The effect of different ratios on the properties of porous ceramics.

Based on the influence of different raw material ratios on the properties of the porous ceramics, the A2 ratio—comprising sludge, gasification slag, glass wool, shale, and waste alkaline solution in a 5:2:1:1:1 ratio—was determined to produce the optimal performance in the resulting porous ceramics.

Influence of Sintering Temperature on the Properties of Porous Ceramics

Based on a raw material ratio of 5:2:1:1:1, the effects of different sintering temperatures on the properties of porous ceramics were investigated. As shown in Fig. 4a, the apparent porosity of the porous ceramics initially increases and then decreases with rising temperature. At 1000 °C, the apparent porosity is 58.4%, which may be attributed to unreacted free carbon residues. When the temperature increases to 1100 °C, the diffraction peaks of mullite ($3Al_2O_3 \cdot 2SiO_2$) and anorthite ($CaAl_2Si_2O_8$) are significantly enhanced (Fig. 6), indicating that the solid-state reactions are approaching completion and a stable grain boundary structure is formed. At this point, the apparent porosity increases to 68.2%. Fig. 3b shows the water absorption of porous ceramics at different sintering temperatures. At 1100 °C, the water absorption reaches 57.12%, followed by a downward trend, which corresponds with the trend in apparent porosity. This is due to the expansion of the liquid phase area at higher temperatures, which fills the smaller pores in the product and leads to greater particle bonding, resulting in a decrease in both porosity and water absorption at higher temperatures [13]. Fig. 3c illustrates the compressive strength of the porous ceramics at various sintering temperatures. As shown, the compressive strength increases with temperature, rising from 10.56 MPa at 1000 °C to 19.89 MPa at 1200 °C. This improvement is attributed to the formation of more molten phases at higher temperatures, which reduce porosity, lower the apparent pore rate, and enhance densification—thereby increasing compressive strength. Meanwhile, the enhancement in compressive strength is intimately correlated with microstructural evolution (as depicted in Figs. 4c and 7). In the temperature range of 1000–1100 °C, high-temperature conditions facilitate the formation of sodic-calcium feldspar and mullite phases from SiO_2 and Al_2O_3 (Fig. 6). The liquid phase infiltrates the pore network, reinforcing grain boundaries—SEM observations reveal that the A2 group exhibits increased pore wall thickness at 1100 °C (lower right panel of Fig. 7). As the temperature rises to 1100–1200 °C, the liquid phase content further increases, promoting densification. Concomitantly, the porosity decreases from 68.2% to 54.3%, accompanied by a corresponding increase in compressive strength from 19.89 MPa to 24.5 MPa. Fig. 3d shows the bulk density of the porous ceramics across

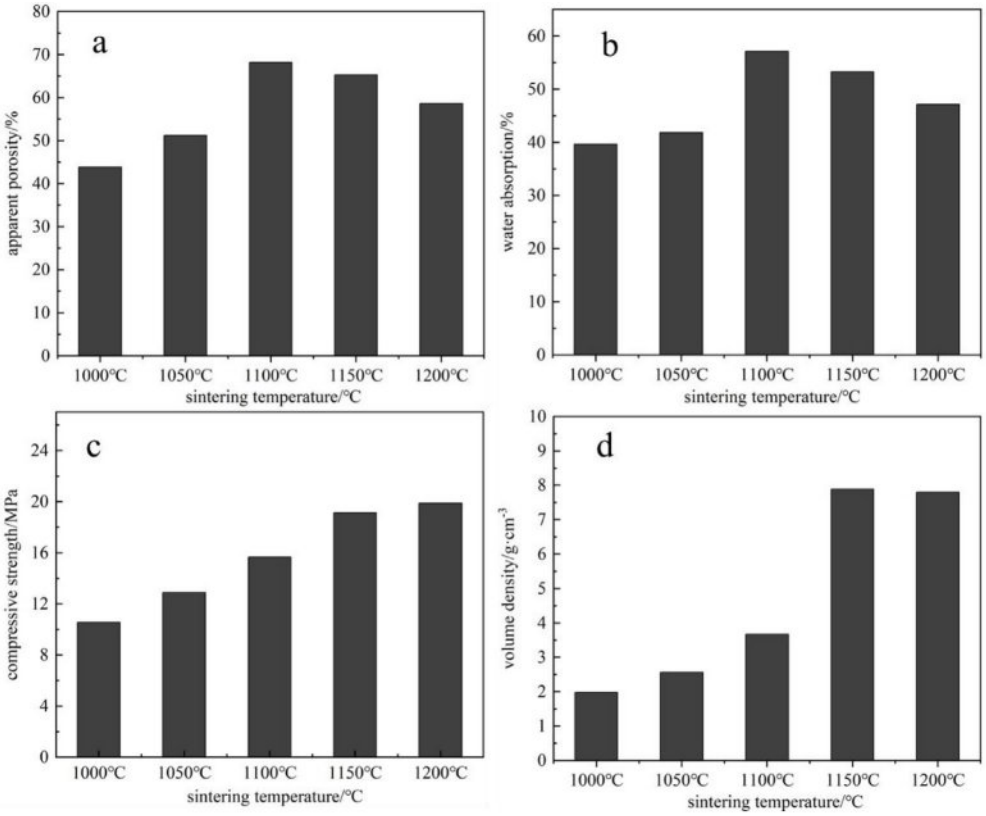

Fig. 4. The effect of sintering temperature on the properties of porous ceramics.

different sintering temperatures. It can be observed that from 1000 °C to 1150 °C, the bulk density remains relatively low. This may be due to insufficient particle bonding and the presence of large and numerous pores at lower temperatures, resulting in a looser ceramic structure. As the temperature rises and reaches 1150 °C, the bulk density begins to increase significantly, showing a gradual upward trend. This is caused by enhanced diffusion and fusion among ceramic particles at higher temperatures, leading to reduced porosity and improved densification, thereby increasing the bulk density. In conclusion, based on the influence of sintering temperature on the properties of porous ceramics, 1100 °C is identified as the optimal sintering temperature.

Influence of Holding Time on the Properties of Porous Ceramics

Based on a raw material ratio of 5:2:1:1:1 and a sintering temperature of 1100 °C, the influence of different holding times on the properties of porous ceramics was investigated. As shown in Fig. 5a, when the holding time is 4 hours, both the apparent porosity (67.8%) and the compressive strength (65.8 MPa) reach their peak values, indicating that grain growth becomes more uniform at this stage. With further extension of the holding time, secondary recrystallization intensifies, and grain boundary migration leads to a reduction in porosity, which drops to 54.3%. This is because prolonged holding allows for more thorough fusion between particles, filling some of the pores and thereby reducing the apparent porosity. Fig. 5b shows the water absorption of porous ceramics under different holding times. The trend mirrors that of the apparent porosity. At 4 hours, the water absorption is 65.89%. As the porosity decreases, the capacity for water absorption also diminishes accordingly. Fig. 5c illustrates the compressive strength of the porous ceramics at various holding times. At a holding time of 4 hours, the compressive strength significantly increases to 65.78 MPa. As the holding time continues to extend, the reaction within the ceramic body becomes more complete, resulting in an increased liquid phase [14]. This leads to higher viscosity, fewer pore formations, and enhanced densification of the porous ceramic, thereby progressively improving its compressive strength. Fig. 5d presents the bulk density of porous ceramics at different holding times. The trend aligns with that of the compressive strength—bulk density increases continuously as the holding time is extended. In summary, based on the effects of different holding times on the properties of porous ceramics, a holding time of 4 hours is identified as the optimal duration.

Phase Composition of Porous Ceramics

Figure 6 presents the XRD diffraction patterns of porous ceramics prepared with different raw material ratios. As shown in the figure, multiple characteristic

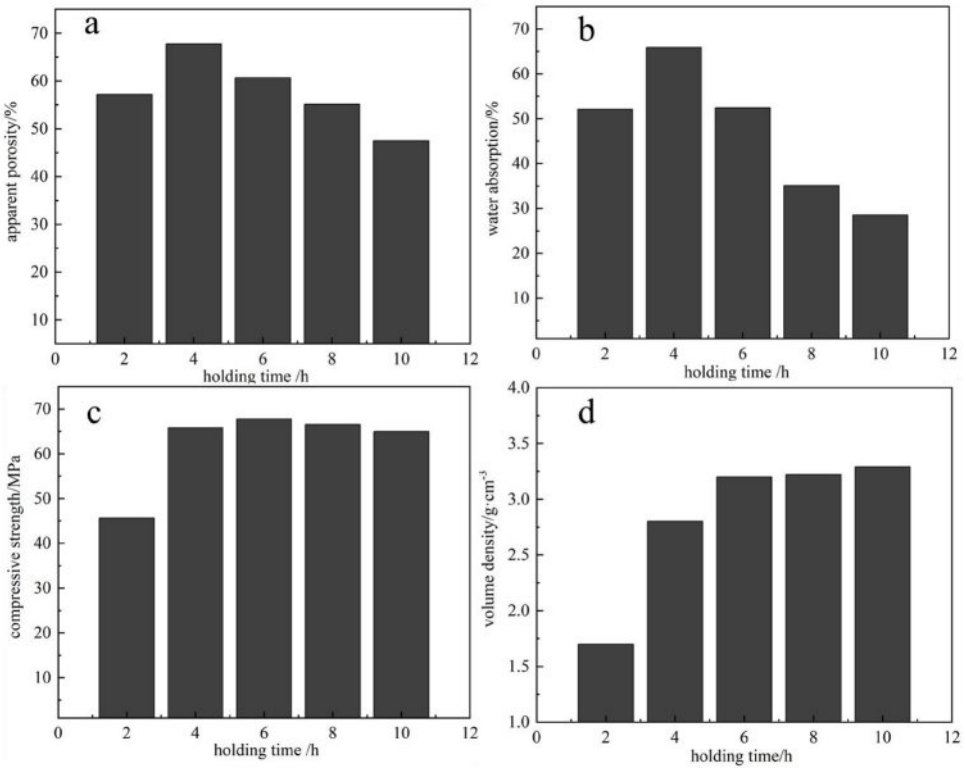

Fig. 5. Effect of holding time on the properties of porous ceramics.

peaks appear, corresponding to different crystalline structures. The porous ceramics produced with varying ratios are primarily composed of Soda-lime feldspar ($[Ca,Na][Al,Si]_2Si_2O_5$), mullite (Al_2O_3-SiO_2), hematite (Fe_2O_3), and a small amount of wollastonite ($Ca(Mg,Al)(Si,Al)_2O_6$). These crystalline phases are bonded by a liquid phase, which helps form the framework of the sample, ensuring relatively stable physical and chemical properties [7]. When the material ratio is A2, the quartz phase gradually disappears, while new solid phases such as sodium-calcium feldspar ($[Ca,Na][Al,Si]_2Si_2O_5$) and mullite (Al_2O_3–SiO_2) emerge and increase in quantity. Compared with other material ratios, the solid-phase diffraction peaks of sodium-calcium feldspar and mullite are more pronounced, indicating a higher content of these crystalline phases. Meanwhile, the liquid phase is further reduced, leading to smaller pore sizes and increased pore wall thickness in the resulting porous ceramics. As a result, both porosity and water absorption decrease, while bulk density and flexural strength increase [15]. The formation of the mullite phase is likely due to a solid-state reaction between alumina (Al_2O_3) and silica (SiO_2) during the high-temperature sintering process [16]. Mullite possesses excellent high-temperature mechanical properties and thermal stability, and its presence enhances the structural stability of the porous ceramics under elevated temperatures [17]. In addition, the XRD patterns of the prepared porous ceramic samples exhibit

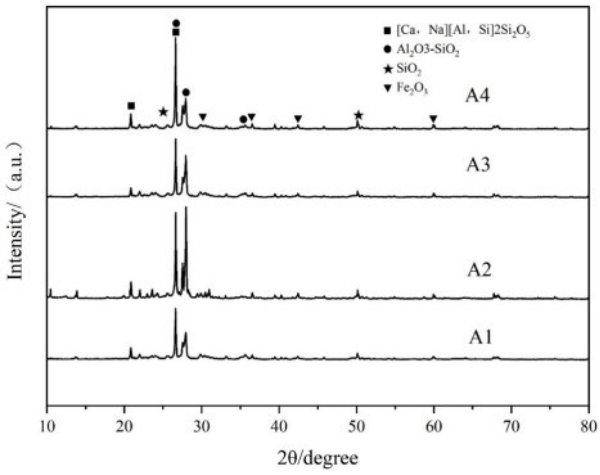

Fig. 6. XRD patterns of porous ceramics.

broad diffuse peaks within the diffraction angle range of 20°–30°, indicating a significant presence of glassy phases in the samples [8]. Specifically, Na^+ and K^+ ions in the waste alkali solution form stable crystalline phases such as albite with SiO_2 during the sintering process. The absence of free alkali peaks in the XRD pattern confirms the complete solidification of alkali components.Semi-quantitative XRD analysis reveals that the amorphous glassy phase accounts for approximately 80% of the total composition of the porous ceramic samples.

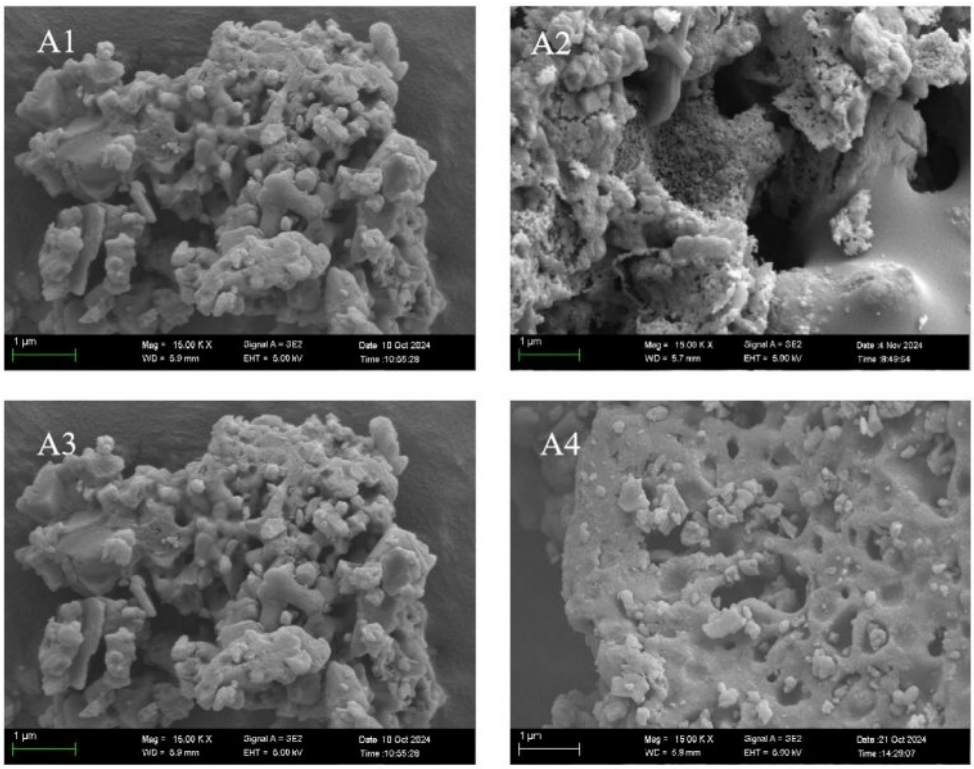

Fig. 7. Microstructure of porous ceramics.

Microstructure of Porous Ceramics

The microstructure of the porous ceramics is shown in Fig. 7. When the raw material ratios are A1 and A3, the amount of solid silicate crystalline phases increases, while the slag phase decreases. As the solid content increases, the viscosity of the ceramic matrix also rises, leading to thicker pore walls. This results in a less ideal porous structure and relatively low ceramic strength. When the raw material ratio is A4, the sample is primarily composed of liquid slag with a small amount of solid quartz and solid sodium calcium silicate ($Na_2Ca_3Si_6O_{16}$) crystals. The porous structure resembles remelted glass, and the main phase is an amorphous slag. Consequently, the ceramic strength is low, and porosity is high [9]. In contrast, when the raw material ratio is A2, the porous ceramic exhibits a typical "honeycomb–skeleton" composite structure. The solid quartz phase disappears, and new solid phases such as sodium feldspar and calcium feldspar appear and increase in quantity. With the increase of silicate crystalline phases and the reduction of the liquid slag phase, the pore size of the ceramic gradually decreases, and the pore wall thickness increases. As a result, the porosity and water absorption of the porous ceramic decrease, while the bulk density and compressive strength increase. As shown in the figure, the ceramic skeleton is relatively dense and forms a continuous network that supports the overall structure. This type of structure contributes to a higher specific surface area of the porous ceramic material, thereby enhancing its adsorption capacity and catalytic performance [10].

Conclusion

This study successfully developed porous ceramic materials using sludge, gasification slag, shale, glass wool, and waste alkali solution as raw materials. A systematic investigation was conducted to examine the effects of raw material ratios, sintering temperature, and holding time on the performance, phase composition, and microstructure of the resulting ceramics.

Raw Material Ratio: The optimal performance was achieved with a raw material ratio of sludge:gasification slag:glass wool:shale:waste alkali solution = 5:2:1:1:1 (designated as A2). Under this ratio, the apparent porosity of the porous ceramics reached 67.89%, with a water absorption rate of 59.57%. Both compressive and flexural strengths showed outstanding performance among all tested ratios, while the bulk density remained within an appropriate range. This is attributed to the well-balanced formation of pore structures and solid/liquid phase proportions during high-temperature sintering, which laid a solid foundation for the subsequent optimization of material properties.

Sintering Temperature: Sintering temperature had a significant impact on the performance of the porous ceramics. An optimal temperature of 1100 °C resulted in an apparent porosity of 68.17% and a water absorption

rate of 57.12%. At this temperature, the densification of the ceramics improved while maintaining sufficient porosity. The compressive strength increased from 10.56 MPa at 1000 °C to 19.89 MPa. Beyond 1150 °C, bulk density increased significantly due to enhanced particle fusion and liquid phase generation at higher temperatures, which contributed to the optimization of pore structure and overall material integrity.

Holding Time: A holding time of 4 hours was found to be optimal. At this duration, the apparent porosity reached 67.78% and the water absorption rate was 65.89%. With prolonged holding time, particle fusion filled more pores and increased liquid phase formation, thereby enhancing the material's densification. As a result, compressive strength improved significantly, and bulk density increased accordingly. These results indicate that a 4-hour holding period fully activates the reaction potential of the raw materials and enhances the overall performance of the porous ceramics.

This research provides key technical parameters and theoretical support for the resource utilization of solid waste in the production of porous ceramics. It effectively addresses challenges in solid waste disposal, reduces production costs, and delivers both environmental and economic benefits. Future research may focus on expanding the variety of raw materials, optimizing processing techniques, exploring synergistic mechanisms among multiple types of solid waste, and refining performance regulation theories to promote the industrial application of this technology and support the implementation of sustainable development strategies.

References

1. H. Duan, Y. Chen, J. Cai, and J. Yang, Acta Sci. Circumstant. 43[4] (2023) 1-10.
2. J. Yang, X. Chen, Q. Sun, S. Zheng, Y. Shen, and M. Zhan, Environ. Sanit. Eng. 32[2] (2024) 63-68.
3. A.I. Harir, R. Kasim, and B. Ishiyaku, Int. J. Sci. Res. Publ. 5[4] (2015) 1-8.
4. F. Han, Z. Zhong, F. Zhang, W. Xing, and Y. Fan, Ind. Eng. Chem. Res. 54[1] (2015) 226-232.
5. T. Wang, B. Wang, B. Hou, Z. Shi, J. Yang, H. Xia, J. Wang, H. Wang, and J. Yang, China's Refract. 29[4] (2020) 10-18.
6. Z. Liu, J. Wang, Z. Zhao, Q. Yang, L. Qin, K. Zhang, X. Wang, N. Su, T. Wen, L. Yuan, and J. Yu, Materials 16[16] (2023) 5679.
7. Y. Zhao, Q. Zhang, J. Chen, Y. Yi, M. Zhou, and J. Cui, J. Mater. Sci.: Mater. Electron. 35 (2024) 1-9.
8. X. Ma, C. Yang, S. Song, X. Song, and X. Mao, Ceram. 32[2] (2024) 107-111.
9. Z. Liu, H. Lan, C. Hu, X. Qiu, and N. An, China Ceramics 60[21] (2024) 50-55.
10. W. Huang, X. Wu, Z. Lin, M. Huang, Y. Jiang, G. Wen, and F. Chen, Shandong Chemical Industry 53[3] (2024) 106-109.
11. Z.H. Wen, Y.S. Han, L. Liang, and J.B. Li, Mater. Charact. 59[9] (2008) 1335-1338.
12. R. Salomao, C.C. Arruda, V.C. Pandolfelli, and L. Fernandes, J. Eur. Ceram. Soc. 41[4] (2021) 2923-2937.
13. M. Dittmer, C. Ritzberger, M. Schweiger, V. Rheinberger, M. Wörle, and W. Höland, J. Non-Cryst. Solids 384[2] (2014) 55-60.
14. S. Li, N. Li, and Y. Li, Ceram. Int. 34[5] (2008) 1241-1246.
15. C. Li, Y. Zhou, Y. Tian, Y. Zhao, K. Yang, G. Li, and Y. Chai, Ceram. Int. 45[5] (2019) 5613-5616.
16. C. Oelgardt, J. Anderson, J.G. Heinrich, and G.L. Messing, J. Eur. Ceram. Soc. 30[3] (2010) 649-656.
17. M. Mouiya, A. Bouazizi, A. Abourriche, Y. El Khessaimi, A. Benhammou, Y. El hafiane, Y. Taha, M. Oumam, Y. Abouliatim, A. Smith, and H. Hannache, Res. Mater. 4 (2019) 100028.